Optics Communications 287 (2013) 245–249

Contents lists available at SciVerse ScienceDirect

Optics Communications

journal homepage: www.elsevier.com/locate/optcom

# Nanowire based hybrid plasmonic structures for low-threshold lasing at the subwavelength scale

Yusheng Bian [a], Zheng Zheng [a,*], Xin Zhao [a], Lei Liu [a], Jiansheng Liu [a], Jinsong Zhu [b], Tao Zhou [c]

[a] School of Electronic and Information Engineering, Beihang University, 37 Xueyuan Road, Beijing 100191, China
[b] National Center for Nanoscience and Technology, No. 11 Zhongguancun Beiyitiao, Beijing 100190, China
[c] Department of Physics, New Jersey Institute of Technology, Newark, NJ 07102, USA

ARTICLE INFO

*Article history:*
Received 26 February 2012
Accepted 19 September 2012
Available online 4 October 2012

*Keywords:*
Nanolasers
Surface plasmon
Optical waveguides

ABSTRACT

Novel plasmonic nanolaser structures are proposed by leveraging the efficient guiding properties of hybrid plasmonic modes of nanowire based waveguides. Theoretical investigations reveal that the coupling between the metal nanowire and the high-index dielectric nanostructure with optical gain results in strong field enhancement in the low-index gap region, sufficient modal overlap with the gain medium and low propagation loss, which could enable lasing at the subwavelength scale with low pump threshold. The proposed nanowire-based plasmonic nanolasers are also compatible with standard fabrication technology and could be appealing candidates for active photonic systems.



## 1. Introduction

Photonic technologies based on nanowires have attracted substantial attention during the last decade [1]. Due to their fascinating optical and electronic properties, nanowires could serve as promising building blocks for novel miniaturized photonic and optoelectronic devices with applications from waveguiding to light emitting [2–4]. In particular, semiconductor nanowires, due to their large refractive-index contrast, have been used to realize efficient miniaturized lasing sources [5]. Although modern bottom-up synthesis techniques enable the fabrication of various kinds of nanowires of different materials with accurately controlled dimensions and shapes, further reduction of the modal dimensions of the corresponding nanowire lasers is still restricted by the diffraction limit.

Recently, several sub-diffraction-limit nanolasers that utilize the surface plasmon (SP) effect as the optical guiding mechanism have been successfully demonstrated [6–8]. For the 2-D plasmonic lasers in [6,8], the hybrid plasmonic structures play an important role in determining their characteristics. As the hybrid plasmonic modes' properties are strongly influenced by the corresponding SPP modes [6,9–25], employing a novel metal nanostructure may result in dramatically modified modal behavior and thus lead to different lasing properties. However, the extra step to fabricate complicated metal structures could greatly increase the fabrication complexity. Here in this paper, we would like to explore the potential to leverage the plasmonic guiding capability of the metal nanowires made by the bottom-up approaches. The interaction between the metal nanowire and dielectric nanostructure could result in a strongly coupled hybrid plasmonic mode as well as a laser cavity for an aligned pair of nanowires. The resultant hybrid mode features both nano-size mode area, sufficient modal overlap with the gain medium and low transmission loss, which are important for low-threshold lasing at the deep-subwavelength scale.

In the following sections, the characteristics of two types of nanowire-based plasmonic nanolasers are investigated in detail. The first type consists of a coupled nanowire pair formed by a gain nanowire and a core/shell metal/dielectric nanowire. The second one is a coaxial waveguide consisting of a metal nanowire surrounded by low–high index dielectric layers. The properties of the nanolasers are investigated by the finite-element method (FEM) using COMSOL$^{TM}$ at the lasing wavelength of 490 nm [6].

## 2. Coupled nanowire pairs based plasmonic laser structure and its optical properties

The geometry of the first type nanolaser is shown in Fig. 1(a). The metallic nanowire is covered with a nanometer-thick low-index cladding, with a high-index semiconductor nanowire attached to its side as the gain medium. Such nanowire pairs could be fabricated by using the self-assembly techniques [26]. The low-index shell of the metal nanowire then forms a natural gap between the gain medium and the metal, enabling the hybrid plasmonic guiding mechanism. The example of the structure considered here consists of a $MgF_2$ coated Ag nanowire sitting on a $MgF_2$ substrate, with a high-index CdS nanowire placed on

* Corresponding author. Tel./fax: +86 10 82317220.
*E-mail address:* zhengzheng@buaa.edu.cn (Z. Zheng).

0030-4018/$ - see front matter © 2012 Elsevier B.V. All rights reserved.
http://dx.doi.org/10.1016/j.optcom.2012.09.043

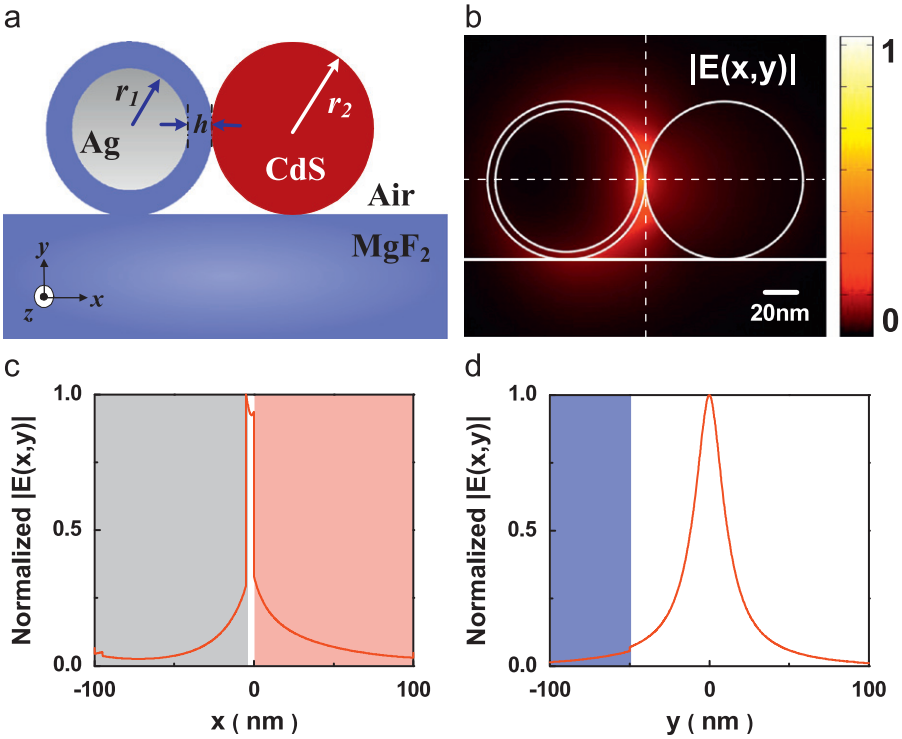


**Fig. 1.** (a) Geometry of the proposed coupled nanowire pairs based nanolaser. (b)–(d) Normalized electric field distribution of the fundamental hybrid plasmonic mode of the proposed structure ($r_1$=45 nm, $r_2$=50 nm, $h$=5 nm).

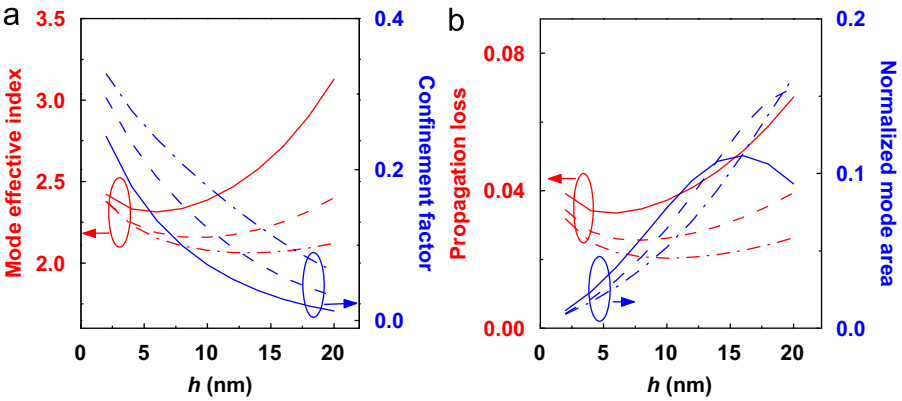


**Fig. 2.** (a) Modal effective index and effective propagation loss. (b) Normalized mode area and confinement factor of the hybrid fundamental plasmonic mode at different $h$: $r_2$=40 nm (solid curve), $r_2$=50 nm (dashed curve), and $r_2$=60 nm (dash–dotted curve).

its right side. Here we choose the silver nanowire because of its good optical properties and atomically smooth surface for low propagation loss [27]. The thickness of $MgF_2$ cladding around the Ag nanowire is defined as $h$. The radii of the silver and CdS nanowires are $r_1$ and $r_2$, respectively. We assume $r_2=r_1+h$. The permittivities of $MgF_2$, CdS and Ag are 1.96, 5.76 and $-9.2+0.3i$ [28], respectively.

Electric field distributions of the hybrid mode shown in Fig. 1(b)–(d) indicate that the lateral coupling between the two nanowires causes strong field enhancement in the nanometer-size gap region, with sufficient modal overlap in the CdS nanowire to provide the needed gain. The mode characteristics including the modal effective index ($n_{eff}$), effective propagation loss ($\alpha_{eff}$), normalized mode area ($A_{eff}/A_0$) and confinement factor ($\Gamma$) of the hybrid plasmonic mode of our proposed structure are shown in Fig. 2 (a) and (b). The effective mode area is calculated using $A_{eff}=(\iint|E|^2\,dx\,dy)^2/(\iint|E|^4\,dx\,dy)$. $A_0$ is the diffraction-limited mode area and defined as $\lambda^2/4$. The confinement factor ($\Gamma$) is defined as the ratio of the electric energy in the CdS nanowire to the total electric energy of the mode. Fig. 2 indicates that, when the gap width $h$ varies from 2 nm to 20 nm, both the mode effective index and the propagation loss decrease first at small gap width, mainly due to the weakened optical coupling between two nanowires. However, when the gap gets relatively large, $n_{eff}$ and $\alpha_{eff}$ will increase simultaneously. That is because more field is confined and located around the Ag nanowire surface when the Ag nanowire is relatively small compared to the gap width. When this effect becomes dominant, it leads to increased effective index and higher loss. It is also shown that reducing the gap size lowers the normalized mode area and enhances the confinement factor in most cases, as the overlap of the hybrid mode and the gain region increases. Only when the nanowire is

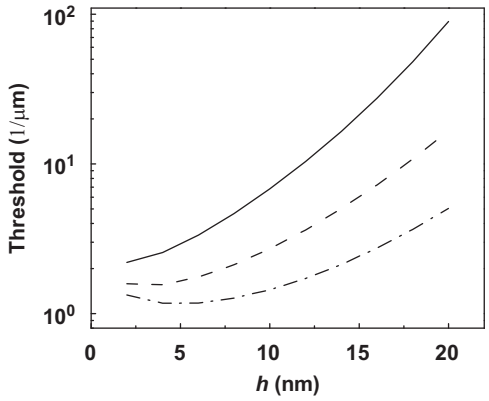


**Fig. 3.** Dependence of lasing threshold on $h$: $r_2$=40 nm (solid curve), $r_2$=50 nm (dashed curve), and $r_2$=60 nm (dash-dotted curve).

rather small (e.g. $r_2$=40 nm), this trend is no longer valid and the mode area may decrease at large $h$. It is also observed that when the gap width is within the range of 2–20 nm, the normalized mode areas are always below 0.2, indicating good deep-subwavelength mode confinement. Fig. 2(a) and (b) also illustrates that for the case of larger CdS nanowire, lower propagation loss and higher confinement factor can be achieved simultaneously.

Based on the above analysis of modal characteristics, we investigate the lasing threshold of the fundamental hybrid plasmonic mode. The nanowire length $L$ is set to be 30 μm and the reflectivity $R=(n_{eff}-1)/(n_{eff}+1)$. The threshold is calculated using $g_{th}=(k_0\alpha_{eff}+\ln(1/R)/L)/\Gamma(n_{eff}/n_{wire})$ [29]. Fig. 3 shows the thresholds of the hybrid mode at various gap widths. It is noted that when the gap width grows from 2 nm to 20 nm, the threshold decreases first before increasing for larger CdS nanowires (e.g. $r_2$=50 nm, 60 nm), indicating a minimal lasing threshold

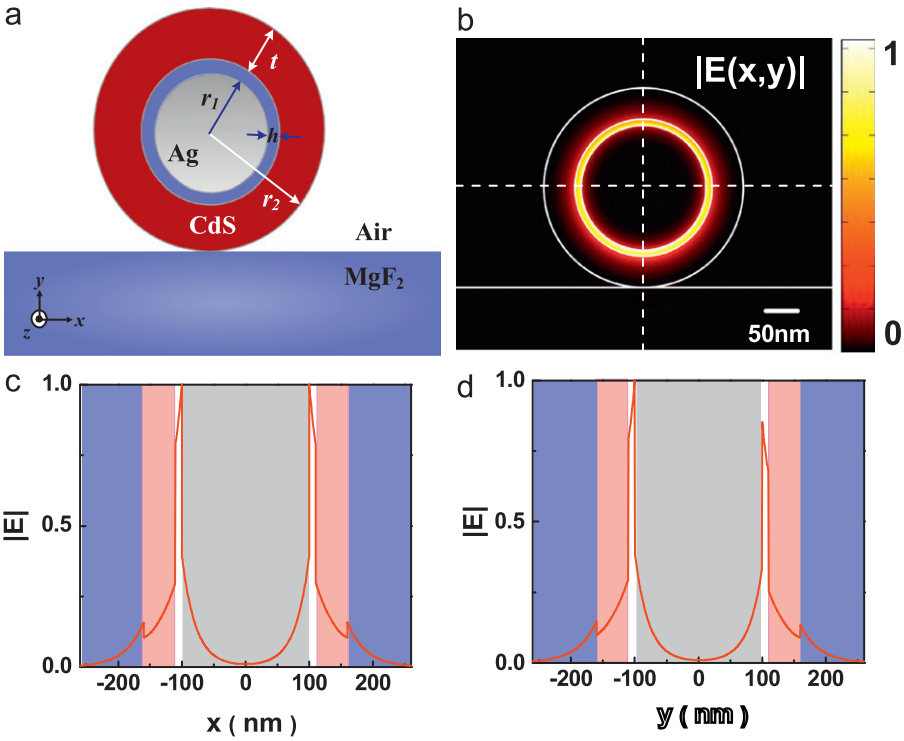


**Fig. 4.** (a) Geometry of the proposed coaxial nanowires based nanolaser. (b)–(d) Normalized electric field distribution of the fundamental hybrid plasmonic mode of the proposed structure ($r_1$=100 nm, $t$=50 nm, $h$=10 nm).

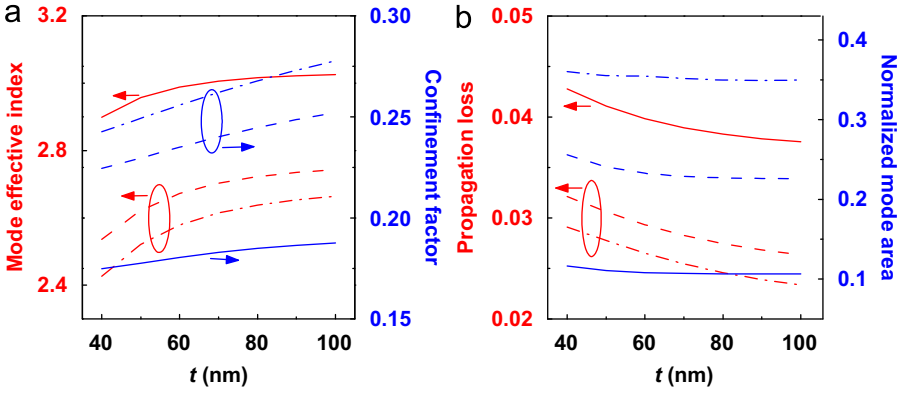


**Fig. 5.** (a) Modal effective index and effective propagation loss. (b) normalized mode area and confinement factor of the hybrid fundamental plasmonic mode at different $t$ ($h$=10 nm): $r_1$=50 nm (solid curve), $r_1$=100 nm (dashed curve), and $r_1$=150 nm (dash–dotted curve).

achieved at a certain gap width. It is also indicated that when the CdS nanowire is small (e.g. $r_2=40$ nm) and the gap width is relatively large, the threshold could see a sharp increase due to the huge propagation loss and weak modal overlap in the gain medium, which is undesirable in practical applications.

## 3. Coaxial nanowire based plasmonic laser structure and its optical properties

Fig. 4 shows the geometry of the second type of plasmonic nanolaser, which consists of a coaxial CdS–$MgF_2$–Ag nanowire positioned on a $MgF_2$ substrate. The radius of the silver is $r_1$, while the thicknesses of the $MgF_2$ and CdS layers are $h$ and $t$, respectively. A Similar waveguiding structure was investigated at the telecom wavelength in [19]. The corresponding electric field distributions of the fundamental hybrid plasmonic mode exhibit a ring-type field distribution with strong field enhancement in the $MgF_2$ layer, as can be seen in Fig. 4(b)–(d). Firstly, we investigate the effect of the thickness of the CdS layer ($t$) on the modal characteristics, where $t$ is set within the range of 40–100 nm. The simulation results shown in Fig. 5 illustrate that both the effective index and the energy confined in the gain medium increase with increasing CdS layer thickness. Meanwhile, lower propagation loss and smaller mode area could also be observed with thicker CdS layer. It is thus expected that better lasing property could also be achieved when $t$ is larger.

Calculation of the lasing threshold reveals a monotonic reduction with increased thickness of CdS layer. Fig. 6 also illustrates that the structure with a larger metallic nanowire requires a lower pumping threshold. Therefore, in order to reduce the threshold, larger $t$ and $r_1$ should be employed. However, for practical applications, some issues such as an increased physical size and undesired effect of other plasmonic mode should also be considered when choosing the dimensions of the CdS layer and the metal nanowire.

Finally, the effect of the thickness of the $MgF_2$ layer is investigated, where $h$ varies from 2 to 20 nm. Fig. 7 reveals that for all the chosen CdS thickness, widening $h$ results in decreased effective index and confinement factor, as well as dramatically reduced propagation loss. Although the corresponding mode area undergoes an increase with extended propagation length, it always stays below 0.4, indicating subwavelength mode confinement. For the lasing threshold, significantly reduced $g_{th}$ is observed with increased $h$, as seen in Fig. 8.

## 4. Conclusion

In this paper, we have proposed and investigated two types of plasmonic nanolasers based on nanowires. Simulation results reveal that for both of the structures, the fundamental hybrid plasmonic mode could be used to realize deep-subwavelength plasmonic laser.

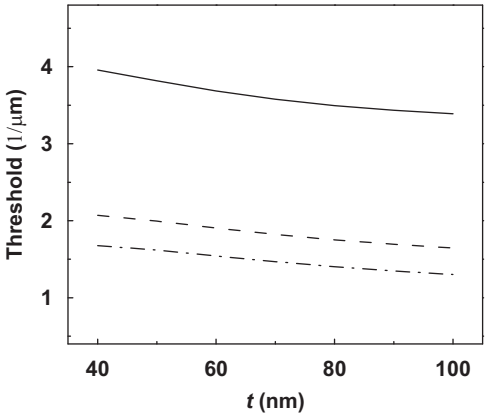


**Fig. 6.** Dependence of lasing threshold on $t$: $r_1=50$ nm (solid curve), $r_1=100$ nm (dashed curve), and $r_1=150$ nm (dash–dotted curve).

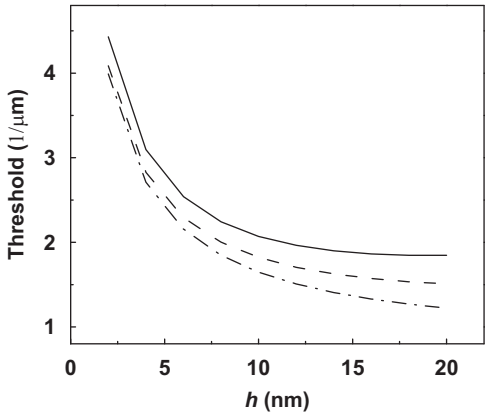


**Fig. 8.** Dependence of lasing threshold on $h$ ($r_1=100$ nm): $t=40$ nm (solid curve), $t=70$ nm (dashed curve), and $t=100$ nm (dash–dotted curve).

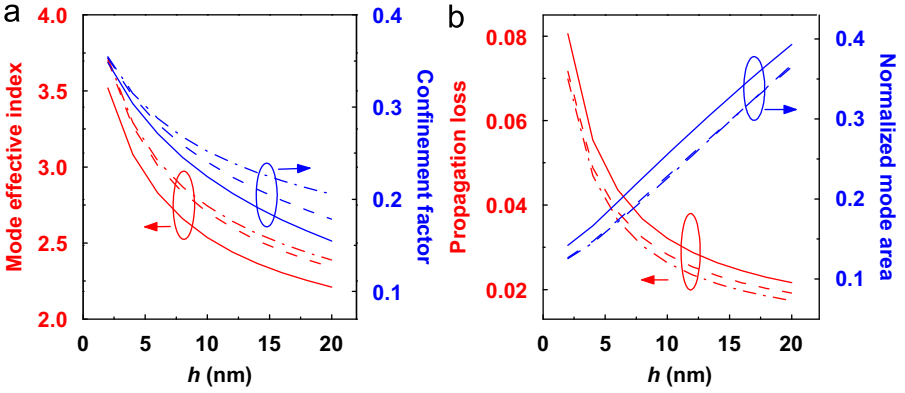


**Fig. 7.** (a) Modal effective index and effective propagation loss. (b) Normalized mode area and confinement factor of the hybrid fundamental plasmonic mode at different $h$ ($r_1=100$ nm): $t=40$ nm (solid curve), $t=70$ nm (dashed curve), and $t=100$ nm (dash–dotted curve).

## Acknowledgments

.The work at Beihang University was supported by 973 Program (2009CB930701), NSFC (60921001/61077064), National Key Scientific Instruments and Equipment Development Special Fund Management (2011YQ0301240502), and the Innovation Foundation of BUAA for PhD Graduates.

## References

[1] R.X. Yan, D. Gargas, P.D. Yang, Nature Photonics 3 (2009) 569.
[2] J. Takahara, S. Yamagishi, H. Taki, A. Morimoto, T. Kobayashi, Optics Letters 22 (1997) 475.
[3] H. Ditlbacher, A. Hohenau, D. Wagner, U. Kreibig, M. Rogers, F. Hofer, F.R. Aussenegg, J.R. Krenn, Physical Review Letters 95 (2005) 257403.
[4] Z. Li, F. Hao, Y. Huang, Y. Fang, P. Nordlander, H. Xu, Nano Letters 9 (2009) 4383.
[5] X.F. Duan, Y. Huang, R. Agarwal, C.M. Lieber, Nature 421 (2003) 241.
[6] R.F. Oulton, V.J. Sorger, T. Zentgraf, R.M. Ma, C. Gladden, L. Dai, G. Bartal, X. Zhang, Nature 461 (2009) 629.
[7] M.A. Noginov, G. Zhu, A.M. Belgrave, R. Bakker, V.M. Shalaev, E.E. Narimanov, S. Stout, E. Herz, T. Suteewong, U. Wiesner, Nature 460 (2009) 1110.
[8] Y.S. Bian, Z. Zheng, Y. Liu, J.S. Zhu, T. Zhou, IEEE Photonics Technology Letters 23 (2011) 884.
[9] R.F. Oulton, V.J. Sorger, D.A. Genov, D.F.P. Pile, X. Zhang, Nature Photonics 2 (2008) 496.
[10] R.F. Oulton, G. Bartal, D.F.P. Pile, X. Zhang, New Journal of Physics 10 (2008) 105018.
[11] D.X. Dai, S.L. He, Optics Express 17 (2009) 16646.
[12] Y.S. Bian, Z. Zheng, X. Zhao, J.S. Zhu, T. Zhou, Optics Express 17 (2009) 21320.
[13] J.T. Kim, J.J. Ju, S. Park, M.-s. Kim, S.K. Park, S.-Y. Shin, Optics Express 18 (2010) 2808.
[14] J. Tian, Z. Ma, Q.A. Li, Y. Song, Z.H. Liu, Q. Yang, C.L. Zha, J. Akerman, L.M. Tong, M. Qiu, Applied Physics Letters 97 (2010) 231121.
[15] I. Avrutsky, R. Soref, W. Buchwald, Optics Express 18 (2010) 348.
[16] M.Z. Alam, J. Meier, J.S. Aitchison, M. Mojahedi, Optics Express 18 (2010) 12971.
[17] Y.S. Bian, Z. Zheng, Y. Liu, J.S. Zhu, T. Zhou, Optics Express 18 (2010) 23756.
[18] Y.S. Zhao, L. Zhu, Journal of the Optical Society of America B: Optical Physics 27 (2010) 1260.
[19] D. Chen, Applied Optics 49 (2010) 6868.
[20] Q. Li, M. Qiu, Optics Express 18 (2010) 15531.
[21] Y. Song, M. Yan, Q. Yang, L.M. Tong, M. Qiu, Optics Communications 284 (2010) 480.
[22] Y.S. Bian, Z. Zheng, Y. Liu, J.S. Zhu, T. Zhou, Optics Express 19 (2011) 22417.
[23] Y.L. Su, Z. Zheng, Y.S. Bian, J.S. Liu, J.S. Zhu, T. Zhou, Micro & Nano Letters 6 (2011) 643.
[24] J.T. Kim, IEEE Photonics Technology Letters 23 (2011) 206.
[25] J.T. Kim, Optics Communications 284 (2011) 4171.
[26] Z.H. Nie, D. Fava, E. Kumacheva, S. Zou, G.C. Walker, M. Rubinstein, Nature Materials 6 (2007) 609.
[27] Y.G. Ma, X.Y. Li, H.K. Yu, L.M. Tong, Y. Gu, Q.H. Gong, Optics Letters 35 (2010) 1160.
[28] P.B. Johnson, R.W. Christy, Physical Review B 6 (1972) 4370.
[29] L. Zhu, IEEE Photonics Technology Letters 22 (2010) 535.